Generation of UTC(PTB) as a fountain-clock based time scale

A. Bauch, S. Weyers, D. Piester, E. Staliuniene, W. Yang*

Physikalisch-Technische Bundesanstalt (PTB)

Bundesallee 100, 38116 Braunschweig, Germany

andreas.bauch@ptb.de

* on leave from National University of Defence Technology, ChangSha, PR China

Abstract

The Physikalisch-Technische Bundesanstalt (PTB) has substantially improved the quality of its local time scale UTC(PTB), which is the national realization of the international time reference Coordinated Universal Time (UTC). It serves as basis for PTB's time services, for local clock comparisons and for international time comparisons. Since February 2010 UTC(PTB) has been realized using an active hydrogen maser (AHM) steered in frequency via a phase micro stepper according to an algorithm which combines the frequency comparison data between the AHM and primary and commercial caesium clocks of PTB. Thereby the long-term stability and accuracy of PTB's primary clocks, in particular its fountain clock CSF1, were combined with the short-term frequency stability of the AHM. CSF1 data were used to calculate the steering on all days except of 6 days during 15 months. During the time between July 2010 and July 2011, the time difference between UTC(PTB) and UTC was always less than 6 ns and the monthly mean rate differences never exceeded 0.16 ns/day.

1. INTRODUCTION

The German Units and Time Act entrusts the Physikalisch-Technische Bundesanstalt (PTB) to realize UTC(PTB), a representation of Coordinated Universal Time UTC, as the basis for legal time in the country. As such it is the reference for PTB's time dissemination services, for local clock comparisons and for international time comparisons. According to recommendations of the Consultative Committee for Time and Frequency the deviation of UTC(k) from UTC, where k stands for any laboratory active in this field, should be small, preferably below 100 ns [1]. No unique prescription for the realization of UTC(k) follows thereof, and the various approaches followed world-wide were recently discussed in [2]. For almost 20 years UTC(PTB) used to have its physical representation as standard frequency and one pulse per second (1 PPS) signals based on its thermal beam primary clock CS2 [3] with occasional small frequency steers applied in order to keep UTC(PTB) close to UTC. Already then UTC(PTB) had a good reputation as one of the most long-term stable and predictable time scales world-wide. A deviation from UTC by more than 50 ns occurred only for a few ten days during the last ten years. The day-to-day stability was, however, inferior to that of other timing institutes' time scales realized with hydrogen masers as the signal source. This fact has become even more obvious since two-way satellite time transfer (TWSTFT) and GPS carrier-phase based time transfer have developed as standard methods in the field [4, 5]. A final motivation for a change was a rather technical one: The CS2 ovens were almost depleted of caesium, and clock operation could not be assured beyond some point in time in 2010.

Since February 2010 UTC(PTB) has instead been realized using an active hydrogen maser (AHM) steered in frequency via a phase micro stepper (PMS) as illustrated in

figure 1. This practice enables better use of the resources available at PTB: two cold-atom based caesium fountain clocks, CSF1 [6] and CSF2 [7], two older thermal beam primary clocks, CS1 and CS2 [3], three commercial caesium clocks of type Symmetricom 5071 (high-performance option), and three AHM produced by Vremya-CH. Subsequently we present in more detail the frequency references and infrastructure on which we rely (Section 2) and lay down the algorithm in current use and its practical implementation (Section 3). In Section 4 results are presented. In Section 5 we discuss the potential application of time scale prediction in the context of the development of the timing system for the European navigation system Galileo. A discussion and outlook on further work closes this paper which is an extension of a first presentation of the results in spring 2011 [8].

2. EQUIPMENT USED FOR THE REALIZATION OF UTC(PTB)

2.1. Atomic fountain clock CSF1

The PTB caesium fountain clock CSF1 [6] is in operation since 2000. In CSF1 a 5 MHz quartz oscillator is locked to the central Ramsey fringe of about 0.9 Hz width and a relative frequency instability of 1.4×10^{-13} $(\tau/s)^{-1/2}$ is achieved. The current CSF1 type B uncertainty is lower than 8×10^{-16} (1-σ value).

During the last decade CSF1 has been used in numerous experimental investigations and has been step-by-step further developed. At the same time CSF1 has been used as internal reference for other clocks, mainly the second PTB fountain CSF2, for measurements of optical frequencies (see e. g. [9]), for measuring the scale unit of International Atomic Time (TAI) and, more recently, for the generation of UTC(PTB). The latter two applications require a particularly high level of reliability and availability.

In atomic fountain clocks the most critical elements to ensure continuous operation are the laser systems used. In CSF1 two homemade extended cavity laser systems are employed. The first one serves as the master laser for a high-power slave laser which provides the cooling beams and is also used for the detection of the atoms, the second one serves as the repump laser which is also needed in the atom cooling process. While continuous operation for more than 10 days could be demonstrated on several occasions, the usual laser system operation consists in deliberate interruptions of the laser locks after 2-3 days for checking the laser performance and for a readjustment of laser parameters if necessary. These interruptions normally last just a couple of minutes and are done to ensure that unperceived failures of the laser locks become very unlikely.

32 reports about CSF1 measurements of the TAI scale unit were submitted to the Bureau International des Poids et Mesures (BIPM) up to July 2011. The nominal duration of the measurements varied between 15 and 30 days, and since 2004 the actual data taking covered typically more than 99% of these nominal measurement times thanks to optimized laser operation. The dead times of less than 1% were usually caused by deliberate interruptions.

The CSF1 frequency is routinely measured with respect to two PTB hydrogen masers. When CSF1 is involved in investigations regarding frequency shifts or work on the installations is made, data is usually available at least for the nighttime and the weekends.

2.2. Thermal beam clocks

PTB's primary clocks CS1 and CS2 have been operated since 1969 and 1985, respectively. Both share a common construction principle whose genesis was described in [3]. Like in CSF1 a 5 MHz quartz oscillator is locked to the central Ramsey fringe of about 60 Hz width and a relative frequency instability of 85×10^{-15} $(\tau/h)^{-1/2}$ and 60×10^{-15} $(\tau/h)^{-1/2}$, respectively, is obtained. The clocks' type B uncertainty values have been estimated as 9×10^{-15} and 12×10^{-15}, respectively (1-σ values). Both clocks have been designed not only in view of achieving such a low uncertainty but also to enable continuous operation for years. Measurements of the TAI scale unit were provided without gap for 24 years from CS2 until in August 2010 when the atomic beam generation failed because the two caesium ovens (which are alternately in operation) were depleted. CS2 operation was interrupted for three months. It is intended to continue operation of both clocks as steering reference for the UTC(PTB) generation as described in Section 3.

2.3. Measurement infrastructure

Figure 2 gives a simplified view of the measurement infrastructure involved in the UTC(PTB) generation. The realization of the time scale is made in duplicate, named UTC(PTB) and UTH(PTB). The output frequency of an AHM is steered using a phase micro stepper (PMS) (Spectra Dynamics Inc. HROG-5). The PMS allows the introduction of a fractional frequency offset between the input and the output 5 MHz signals with a resolution of 6×10^{-17}. The PMS noise contribution remains lower than that of the typical noise of a AHM as long as the relative offset introduced remains bounded to 2×10^{-13} in magnitude which is fulfilled in our operating scheme. Switching among all signals (5 MHz and 1 PPS) of the two realized time scales requires manual intervention, but is simple to do.

All input data needed for the daily computation of the steering value are generated with long-established measurement infrastructure. A dual channel phase comparator (PCO) (Vremya-CH VCH-314) with a measurement noise of less than 8×10^{-14} $(\tau/s)^{-1}$ for τ up to 10^5 s is used to get hourly mean frequency differences between CSF1 and the two AHMs involved. Actually, the PCO provides output pulses at a rate of $(1+10^6\times\delta f/f_0)$ Hz, where $\delta f/f_0$ represents the relative frequency difference between the two signals compared in one channel at the nominal frequency f_0. The large error multiplication factor of 10^6 allows to measure this 1 Hz output with a standard time interval counter (TIC) retaining the high measurement resolution.

The signal of the 5 MHz quartz oscillator which is part of the CSF1 electronics is permanently provided even if the quartz is deliberately not locked to the CSF1 Ramsey signal or if the regular clock operation fails, e. g., because of a loss-of-lock of one of the lasers used for atom cooling and detection. Using CSF1 data in such a condition would result in the generation of an erroneous steering command. To avoid this, a 1 PPS monitor signal is generated at CSF1 for indicating normal operation. This 1 PPS signal is automatically disabled if the regular fluorescence signal of the atoms trapped in the magneto-optical trap of CSF1 is no more detected. It can be manually disabled to indicate that service work is done on CSF1. If the 1 PPS monitor signal is disabled, the frequency measurement results obtained during the respective periods are automatically excluded from the calculation of the steering value. To implement these interfaces providing the “use – don’t use” information proved as one of the key issues to be solved.

Figure 2 shows also part of the measurement infrastructure linking CS1 and CS2 and the commercial caesium clocks with the two AHMs. In duplicate (not shown), the 1 PPS signals are routed to signal switches and compared by two time interval

counters (TIC). Data from one of the TICs are monthly provided to the BIPM Time Department as PTB's input to the algorithm ALGOS for the calculation of the time scales Echelle atomique libre (EAL) and International Atomic Time (TAI). One consequence of reporting the clock data to BIPM is that monthly rates of the clocks with respect to TAI, rTAI, as well as the statistical weights with which the clocks contributed to EAL, wTAI, are available from the BIPM FTP server [10]. The files containing the most recent rTAI and wTAI values are available immediately after the publication of a new monthly issue of the Circular T.

2.4. Frequency instability of the various frequency standards involved

In figure 3, the frequency instability of the frequency standards so far involved in the project is depicted. It illustrates that the performance of the various devices is quite different. Results of AHM comparisons are shown for the case of a local comparison among two of them with averaging times between 1 s and 10 days (symbol +), and for comparisons of the same two AHM with the time scale UTC(NIST) of the US National Institute of Standards and Technology for averaging times between 1 day and 30 days (symbol $\times$). The lower instability is found for AHM H5 (BIPM code 40 590), the frequency of H8 (BIPM code 40 508) is more variable in the long term. A linear drift was removed from the data in both cases. The performance of the fountain clock CSF1 is shown in full symbols, with respect to an AHM and to an optical frequency standard of PTB [9] with an instability superior to CSF1 and to the AHM. The data span analyzed here is longer than that reported in figure 3 of [9]. These data advised us to steer the maser frequency through the PMS towards CSF1 at least once per day based on daily average values of the frequency difference. The frequency instability of all other available standards equals that of the hydrogen masers only after far more than 10 days of averaging. Thus daily maser steering their

frequencies towards those references has been based on linear fits to a certain number of daily average values collected in the past, extrapolated to the current day.

3. BASIC ALGORITHM DESIGN AND ITS PRACTICAL IMPLEMENTATION

The PMS is commanded daily to shift the 5 MHz input frequency by the relative amount

$$\delta f_{\mathrm{Steer}} = \delta f_{\mathrm{Ref}} + \delta f_{\mathrm{Rate}} + \delta f_{\mathrm{Offset}}. \qquad (1)$$

Here δf_{Ref} is intended to adjust the frequency of the AHM to the rate of the reference clocks and is calculated daily taking into account the frequency instability of the reference clocks involved as just described. The summand δf_{Rate} reflects the reference clock rates with respect to TAI. The third term $\delta f_{\mathrm{Offset}}$ assures the long term steering of UTC(PTB) towards UTC and is currently calculated as $\{UTC\text{-}UTC(PTB)\}_{\mathrm{LRD}}$/60 d, where the time difference is the one of the last reported day (LRD) in the most recent issue of the Circular T. Three optional steering values $\delta f_{\mathrm{Steer}}$ are calculated in parallel each day. Independent of the Option, the last two summands in (1) are in our approach constant between successive issues of the Circular T, only the δf_{Ref} term changes daily.

Option 1: The utilization of one of PTB's most accurate clocks, the fountain clock CSF1, as the reference for the realization of UTC(PTB) seems quite natural. Initial work in this direction started almost 10 years ago [11,12], but was interrupted several times because of a lack of a reliable hydrogen maser or because CSF1 was utilized in various kinds of studies and not suitable as a steering reference. To determine

δf_{Ref}, hourly measured frequency differences between CSF1 and the AHM are used. If during day D-1 six hours of data are available, the mean value, corrected for the daily frequency drift of the maser, is used as δf_{Ref} during day D. The AHM frequency drift is estimated from its behavior with respect to TAI during the last three months using its published rTAI values. Here three months was chosen as a compromise between following the maser performance closely and introducing extra instability, just as it is done in the new frequency prediction algorithm used in the calculation of EAL [13]. When no valid CSF1 data are available for day D-1, the steering for day D is calculated from a linear fit to the preceding three daily values. If less than two such data are available (e.g. two extrapolated, but not measured data), the steering is applied based on one of the other two options. For δf_{Rate} we use d, representing the fractional deviation of the scale interval of TAI from the SI second on the geoid, as published in the last line of Section 4 of the Circular T. In Section 5 alternatives to this choice will be discussed.

Option 2: The AHM frequency is compared to the caesium beam clocks which are all treated identically. No distinction between “primary” and “commercial” is made because their frequency instability is similar and all required data are obtained from the same time interval counter. For each clock $\delta f_{\mathrm{Steer}}$ (1) is calculated daily. In so doing δf_{Ref} is updated based on linear extrapolation of past daily frequency comparison data of the respective clock and the maser involved for an interval adapted to the frequency instability of the respective clock, currently 16 days for CS2 and 25 days for the other four clocks. The monthly published rates rTAI of the individual clock are used for estimating δf_{Rate}. $\delta f_{\mathrm{Offset}}$ is obviously the same for each

clock. The individual results δf_{Steer} are combined using the statistical weights wTAI of the individual clocks.

One issue to be solved was the proper determination of δf_{Rate}. The rTAI(M) values of all clocks involved for the month M were compared to rTAI(M-1), but also to the mean rTAI over the last three and five months, respectively, for a period of two years. There is no clear optimum choice for all clocks involved for predicting rTAI for the current month based on the past. Up to now the mean rTAI value over the three last months was used and combined with the most recent wTAI value. It may not be the optimum choice to treat all clocks in the same way, but for the sake of simplicity this choice was made.

Option 3: Option 2 is calculated a second time, but weight zero is given to all clocks except to the PTB primary clock CS1 until February 2011 and CS2 after that. After the recent maintenance of CS2 this clock has been preferred for Option 3 because of its superior frequency stability.

After midnight the software collecting data from the TIC mentioned before provides daily files containing results (time offsets, clock rates, etc.) of the preceding day. The time scale generation software accesses these files for calculation of δf_{Ref}. In case of Options 2 and 3 the most recent data are combined with data collected on previous days to obtain the frequency prediction of each clock with respect to both AHM. The calculation of the three steering values is performed at 0:25 UTC. The software selects the daily steering value according to pre-selected priorities and availability: Priority 1 has always been given to the use of CSF1 data (Option 1), priority 2 is given to the clock combination result since the required software routine had been

sufficiently tested in October 2010. Before that a simpler software version was running that used a single clock as reference, CS2 alone as Option 2 and CS1 as Option 3. Option 3 has the lowest priority.

The selected value is sent to the PMS a few minutes later. After that the instrument is queried, and proper reception of the command is verified. If none of the three values is available, the PMS retains its previous setting and alarms are distributed. Based on the experiences gained with the steering references, a newly calculated value $\delta f_{\mathrm{Steer}}$ should not deviate from the value calculated one day before by more than 2×10^{-14}. If this condition is not met, the software checks all available optional values. If all show a similar large step, the step according to priority 1 is applied and an alarm is generated, as such a large step would point to a malfunction of the AHM involved. For each option and for each implementation, daily log-files and archive files are produced which allow a check of all calculations after the fact. The directories are searched for the various files by independent software and alarm messages are sent when an expected file has not been produced.

The software supports two events which cannot be excluded to happen. Firstly, based on auxiliary data which are permanently collected, a change between the AHM in use to the third one available in the lab is quickly made in case that service is needed to the AHM in operation. Secondly, the AHMs are equipped with a cavity auto-tuning system, but they nevertheless exhibit a (linear) frequency drift. The synthesizer which is part of the AHM electronics is stepped once in a couple of months as for practical reasons the relative frequency difference between the AHM frequency and that of the fountain clocks should be limited to about 10^{-13}. If this was decided to do, also the previous comparison data on which calculation of all three

optional steering values are built have to be corrected after the fact and the time scale calculation process has to be re-run. The software can be re-started manually at any point in time so that corrected input data can be used to produce a refined steering value in this or other cases. If no software input is available, the frequency steering remains unchanged, and alarms are distributed.

4. RESULTS

4.1. Availability of data

The new realization scheme was implemented after 27 January 2010, corresponding to Modified Julian Day (MJD) 55254. Option 1 became available only about four weeks later. Since then, until July 2011, the frequency steering could be based on Option 1 (CSF1 data) very reliably, only on six days the steering was based on another option. This high amount of availability was achieved because CSF1 was mainly used as a frequency reference for CSF2 evaluations during this period, and only a few intrinsic CSF1 investigations took place. Of course, during many days CSF1 data were usable for less than 24 hours, as one can infer from figure 4. Between March 2010 and July 2011 CSF1 was also used in 10 measurements of the TAI scale unit during which its operation has been ensured with a duty cycle approaching 100%. During such periods, CSF1 operation may be interrupted for just a couple of minutes for a quick check of the lasers, but this entails a loss of the full hour in the time scale generation. This explains the frequent occurrence of 23 data points per day to be seen in figure 4. The results of 9 of these measurements are later shown in figure 11. On very few occasions no $\delta f_{\mathrm{Steer}}$ was produced based on Options 2 and 3, mostly caused by hardware problems of the 1 PPS distribution.

4.2. Comparison to external references

The UTC(PTB) short-term stability improved immediately when the new realization scheme was implemented, as illustrated by a comparison to UTC(NIST) using a GPS carrier phase comparison (NRCan PPP software [14]) whose result is shown in figure 5. More important is the long-term behaviour of the time scale which is judged from data published in Circular T. In figure 6 we compare six months of {*UTC-UTC(PTB)*}, in 2009 - 2010 (CS2 based) and 2010 – 2011 (fountain based), respectively. The improvement in stability and thus predictability is eye-catching. In comparison with other timescales of renown quality, we see in figure 7 that UTC(PTB) is now competitive, despite of the fact, that a rather limited number of clocks has been involved in its realization. During the last 12 months, including July 2011, UTC(PTB) deviated from UTC by less than 6 ns. Another quantitative result is given in figure 8. UTC(PTB) has been continuously compared to UTC(NIST) using TWSTFT, and from the daily measurements, nominally 12, but on average over the last two years 11.7 per day, a nominal time difference at 0:00 UTC has been interpolated for each day. Based on those daily time differences the instability of the underlying time scales was calculated based on two data sets comprising 300 days, one taken before and the other one after the new realization scheme of UTC(PTB) had been implemented. The historical data shown in figure 8 clearly represent the frequency instability of PTB CS2 as explained in Section 2.4. The recent data show a significant improvement, they represent, however, a combination of the frequency instability of both scales involved and of the time transfer. The frequency instability of both time scales with respect to UTC is illustrated also in figure 8.

4.3. Documentation of PTB internal data

In figure 9 we show three optional steering values calculated during one year including June 2011. Option 2 was calculated only since early July 2010 and would have been used only from October 2010 onwards if needed. The values include one intentional frequency adjustment of AHM H5. As a matter of fact, the AHM H5 selected as the physical source of UTC(PTB) behaved quite predictable during the last months. The alternate channel (UTH(PTB)) faced some abnormal events. As mentioned before, UTC(PTB) is independently generated in duplicate, based on two different masers. Switching between the two signals could become necessary for replacement or repair of equipment involved. This is facilitated as both scales are in close agreement as shown in figure 10 which contains three months of data as an example. Additionally, since May 2011 another PMS has been connected to AHM H5 and a test version UTT(PTB) steered with respect to the clock combination (Option 2) with highest priority has been generated.

5. DISCUSSION

5.1. How to relate CSF1 data to the rate of TAI?

From the very beginning of the project, the use of fountain clock data as the reference for steering the AHM frequency was given the highest priority. One issue in debate was the optimum way to determine at all times the relation between CSF1 and the rate of TAI. The decision was made initially to always use *d* estimated for the previous month and published at the end of Section 4 of Circular T, irrespective of the fact that *d* depends in a complicated way on the past contributions of several primary frequency standards [5, 15], not always including CSF1. The motivation was that *d* is available reliably and from the same source of information that has to be looked up anyway to get $\delta f_{\mathrm{Offset}}$. Another choice would have been to rely always on the last published value *d*(CSF1) or a mean value over recent data of that kind. In a

different approach we combined monthly average frequency values $\langle y(\text{CSF1-AHM})\rangle_M$ built from the daily values δf_{Ref} (Option 1), with the monthly values rTAI for the AHM involved to yield y(CSF1-TAI) for a full month, called d_1(CSF1). There are two subtle difficulties involved. As described before, a value $\langle y(\text{CSF1-AHM})\rangle_M$ practically never covers 100 % of a month, but a rTAI value for the AHM does. rTAI-values, on the other hand, do not represent true frequency averages but are calculated by the BIPM from the slope of a linear fit to the seven time difference values reported monthly according to the ALGOS schedule. In view of this another alternative was tested: {*UTC-UTC(PTB)*} from Circular T and local data {*UTC(PTB)-AHM*} were used to calculate the mean frequency differences of the AHM for the period of reporting CSF1 data to BIPM. Combining these with the $\langle y(\text{CSF1-AHM})\rangle$ for the same interval yields another estimate d_2(CSF1). In figure 11 we illustrate that the four options would have lead to steering values differing by a few parts in 10^{-15} in some instances. d(CSF1) and d_2(CSF1) agree typically well within 5×10^{-16}. It is worth recalling that a 1×10^{-15} error in δf_{Rate} persisting for a full month would results in a 2.7 ns increase or decrease in the time scale difference.

The result of one simulation made is shown in figure 12 where the simulated time difference, based on the monthly d_1(CSF1), shows significantly larger deviations from zero as what was achieved in reality. Fortunately, the use of d is the simplest to implement, and as it provided good results up to now this practice will be retained for a while.

5.2. Time Scale Prediction

The capability to predict the time difference {*UTC-UTC(k)*} at a given epoch during the period of time when this information is not available because of the publication of

the Circular T in deferred time, is important when laboratories state a Calibration and Measurement Capability (CMC) in the Key Comparison Data Base maintained by the BIPM [16]. To give an example, PTB stated a few years ago that {*UTC-UTC(PTB)*} could be predicted with 40 ns uncertainty (95% confidence) 20 days after the last published value in Circular T. Inspection of figure 7 reveals that this capability has been substantially improved after the new realization scheme had been implemented.

This is of even more relevance as UTC(PTB) shall be used as one of the time references for the generation or validation of the Galileo System Time (GST) of the European satellite navigation system Galileo [17]. The timing system is at the heart of every navigation system. GST will be realized in two Precise Timing Facilities (PTF). The master PTF will provide GST as a physical signal with properties defined such that the navigation function of Galileo as specified in the Galileo Mission Requirements Document can be fulfilled [18]. GST realized in the slave PTF will be kept in close synchronism to that of the master PTF. As the US Global Positioning System (GPS) is already today, Galileo will become also a time distribution system. The Galileo Time Service Provider (GTSP) will ensure that GST is steered towards UTC. One option to achieve this combines the prediction of {*UTC − UTC(k)*} based on data published in Circular T with measurements of {*GST – UTC(k)*} in quasi real time [19]. The success of this process depends largely on the quality of the local realizations of UTC(k) in the institutes involved.
In figure 13 the results of predicting {*UTC-UTC(PTB)*} during one year are shown. Each prediction spans 45 days beginning with the last data point reported in Circular T. As explained in [19], several options for making the prediction have been implemented in the software developed for the purpose. Here results of the most

appropriate ones are shown. Option 1 is a linear fit (LF) to the (usually) 7 time differences reported in a Circular T and the linear regression is extended over the prediction interval. Option 2 is based on a linear function starting at the last reported point in Circular T with the slope equal to the mean rate over the past month (LPR). The summands $\delta f_{\mathrm{Rate}} + \delta f_{\mathrm{Offset}}$ (1) usually change when the new Circular T is published. This is taken into account in the prediction by adjusting the slope of the linear function. If the predicted values are compared to the values reported one month later, ideally the difference would be zero which of course is not the case. We find for both optional prediction strategies that the deviation between predicted individual and real value is less than ±6 ns at the end of the prediction interval at 45 days. This result is could be expected based on the documented frequency instability in figure 8, and is very favorable in terms of the requirement regarding the prediction of the offset UTC minus Galileo System Time in real time, as reported in [18].

6. Outlook

The availability of fountain clock data was crucial for the success demonstrated in the previous sections. This was concluded from a couple of simulations regarding the situation that one of the other options had to be used at all times instead of Option 1. The simulations included deviations from the practice used hitherto and described in Section III to calculate δf_{Ref} and δf_{Rate}, namely the use of the most recent or a longer average value for rTAI, and also the averaging interval for the calculation of δf_{Ref} was questioned. In all cases a realization of UTC(PTB) based thereon would not have had the quality that was actually achieved using mostly Option 1. Although CSF1 has proven very reliable, it seems worth while searching a closer to optimum algorithm for Option 2, but at the same time limiting the complexity of the software. Only then the

quality of UTC(PTB) can be assured also in case that no fountain data are available for an extended period.

As longer lasting intrinsic investigations and upgrades of CSF1 have been scheduled, the second PTB fountain CSF2 [7] has been prepared to take over the reference role for Option 1. CSF2 has already proven a similarly reliable operation as CSF1. The interfaces between CSF2 and the time-scale generation software were recently implemented, but no use was made thereof yet. Later also a combination of both fountain outputs could be used for the steering process. Another option under discussion is steering of the hydrogen maser more frequently than once per day.

One has to keep in mind that the UTC-UTC(PTB) differences obtained recently are no longer large compared to the uncertainty with which they have been determined [2, 20]. Delay changes in the time transfer equipment have to be avoided or at least have to be corrected for as otherwise they might spoil the quality of the timescale. Periodic calibrations of the signal delays in the time transfer equipment are a proper way to support this [21, 22].

ACKNOWLEDGMENT

The availability of fountain data was instrumental for the success. We gratefully acknowledge valuable support by Vladislav Gerginov and Nils Nemitz to ensure reliable operation of CSF1. Testing and documentation of the software was supported by Jürgen Becker and Thomas Polewka. Yang Wenke thanks China Scholarship Council for funding her one year scholarship in PTB.

DISCLAIMER

PTB as a matter of policy does not endorse any commercial product. The mentioning of brands and individual models seems justified here, because all information provided is based on publicly available material or data taken at PTB and it will help the reader to make comparison with own observations.

REFERENCES

[1] 1993 *Recommendation S5*, Report of the 12th session of the Comité consultative pour la définition de la seconde, 1993

[2] Whibberley P, Davis J and Shemar S, 2011 Local representations of UTC in national laboratories, *Metrologia* **48** S154-64

[3] Bauch A 2005 The PTB primary clocks CS1 and CS2 *Metrologia* **42**, S43–S54

[4] Arias E F and Bauch A 2010 Metrology of time and frequency, in *Handbook of Metrology, M. Gläser and M. Kochsiek, eds., Wiley-VCH, Weinheim*

[5] Arias E F, Panfilo G and Petit G 2011 Timescales at the BIPM *Metrologia* **48** S145-53

[6] Weyers S, Hübner U, Schröder R, Tamm Chr and Bauch A 2001 Uncertainty evaluation of the atomic caesium fountain CSF1 of PTB *Metrologia* **38** 343–52, and Weyers S, Bauch A, Schröder R and Tamm Chr 2001 The atomic caesium fountain CSF1 of PTB *Proceedings of the 6th Symposium on Frequency Standards and Metrology 2001, University of St Andrews, Fife, Scotland, ISBN 981-02-4911-X (World Scientific)* 64–71

[7] Gerginov V, Nemitz N, Weyers S, Schröder R, Griebsch D and Wynands R 2010 Uncertainty evaluation of the caesium fountain clock PTB-CSF2 *Metrologia* **47** 67-79

[8] Bauch A, Staliuniene E, Piester D and Yang W 2011 New Realization Strategy for UTC(PTB) *Proc. Joint IEEE International Freq. Control Symposium and European Frequency and Time Forum, San Francisco 2011* 40 - 43.

[9] Tamm Chr, Weyers S, Lipphardt B and Peik E 2009 Stray-field-induced quadrupole shift and absolute frequency of the 688-THz $^{171}Yb^{+}$ single-ion optical frequency standard *Phys. Rev A* **80** 043403

[10] BIPM *Circular T* http://www.bipm.org/jsp/en/TimeFtp.jsp?TypePub= publication

[11] Weyers S, Hetzel P and Bauch A 2002 Operational Use of PTB's Atomic Caesium Fountain CSF1 *Proc. 16th European Frequency and Time Forum, St. Petersburg 2002*, A-014-A-017

[12] Bauch A, Piester D and Staliuniene E 2005 A new realization strategy for the time scale UTC(PTB) *Proceedings of the 2004 IEEE International Frequency Control Symposium and Exposition* 518 – 523

[13] Panfilo G, Harmegnies A and Tisserand L 2011 A new prediction algorithm for EAL *Proceedings of the 2011 Joint Conference of the IEEE IFCS and EFTF*, San Francisco 2011, 850 - 855

[14] Kouba J and Héroux P 2001 Precise Point Positioning using IGS orbit and clock products *GPS Solutions* **5(2)** 12-28

[15] Petit G 2000 Use of primary frequency standards for estimating the duration of the scale unit of TAI *Proc. 31st Precise Time and Time Interval (PTTI) Systems and Applications Meeting, Dana Point, 1999* 297-304

[16] CIPM *Key Comparison Data Base* http://kcdb.bipm.org/

[17] Achkar J et al 2007 Fidelity – Progress Report on Delivering the Prototype Galileo Time Service Provider *Proc. Joint IEEE IFCS and 21st EFTF, Geneva, 2007* 446-51

[18] Hlaváč R, Lösch M, Luongo F and Hahn J 2006 Timing Infrastructure for Galileo System *Proc. 20th European Frequency and Time Forum, Braunschweig 2006* 391-8

[19] Bauch A, Sen Gupta A and Staliuniene E 2005 Time Scale Prediction Using Information from External Sources. *Proc. 19th European Frequency and Time Forum, Besançon 2005* 448-454

[20] Lewandowski W, Matsakis D, Panfilo G and Tavella P 2006 The evaluation of uncertainties in [UTC-UTC(k)] *Metrologia* **43** 278-86

[21] Feldmann T, Bauch A, Piester D, Rost M, Goldberg E, Mitchell S and Fonville B 2011 Advanced GPS based time link calibration with PTB´s new GPS calibration set-up *Proceedings of the 39th Annual Precise Time and Time Interval (PTTI) Conference, Reston, VA, October 2010*, in press

[22] Piester D, Bauch A, Breakiron L, Matsakis D, Blanzano B, Koudelka O 2008 Time transfer with nanosecond accuracy for the realization of International Atomic Time *Metrologia* **45** 185 – 98

Figure Captions and figures

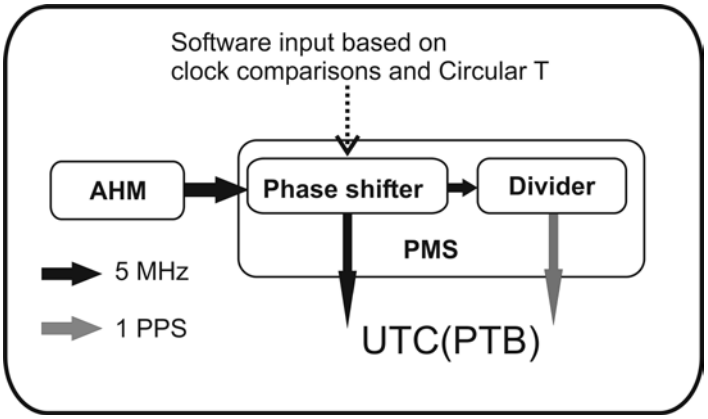

Figure 1. UTC(PTB) realization from an active hydrogen maser (AHM) and a phase micro stepper (PMS).

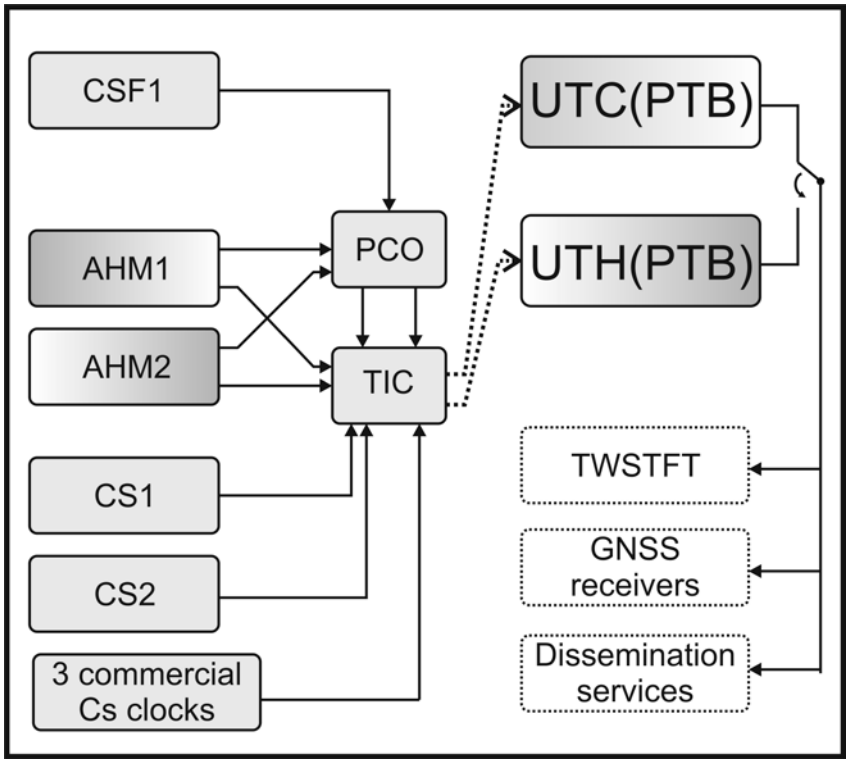

Figure 2. Implementation of duplicate realization of PTB's reference time scale UTC(PTB). Solid lines represent signals (5 MHz or 1 PPS), dashed lines represent data flow to the time scale generation as illustrated in figure 1.

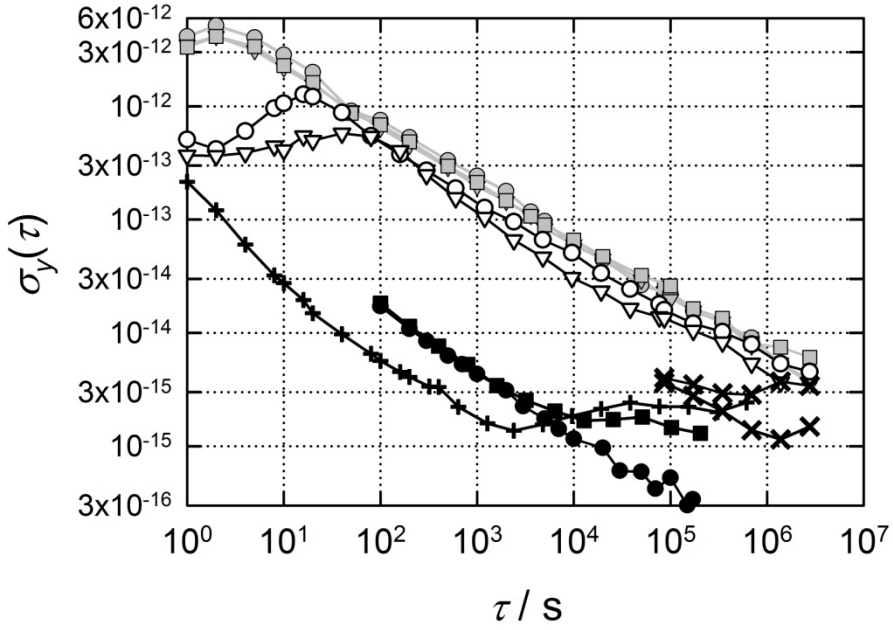

Figure 3. Relative frequency instability of PTB's atomic clocks, AHM instability (+) for a local comparison, (×) for comparison of two masers with UTC(NIST) during one year, CSF1 vs AHM (black squares) and CSF1 vs optical frequency standard (black dots), CS1 (open circles), CS2 (open triangles) and three commercial caesium clocks (grey symbols); reproduced from [8] © 2011 IEEE.

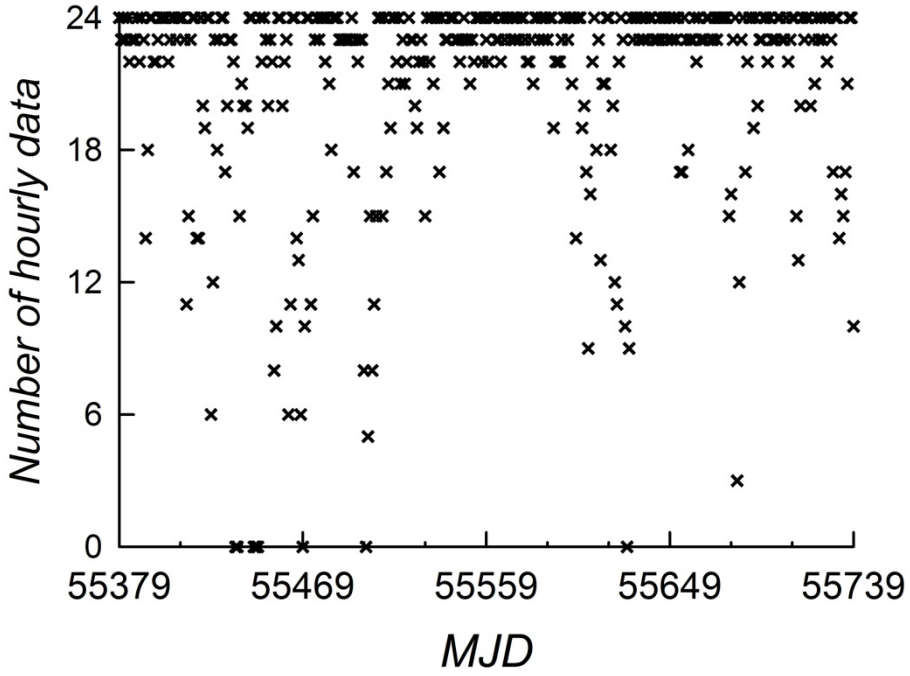

Figure 4. Availability of CSF1 hourly data for the UTC(PTB) generation during one year including June 2011.

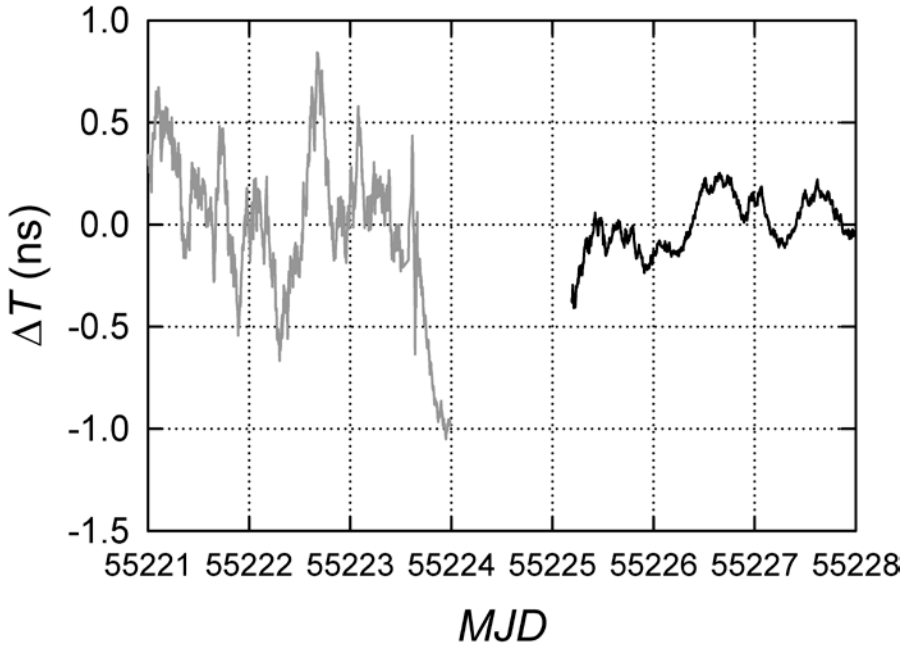

.

Figure 5. Phase comparison UTC(PTB) – UTC(NIST) based on a GPS carrier phase analysis using the NRCan PPP software [13] for a few days before and after the change of the UTC(PTB) realization; individual phase offsets were removed in both data sets before plotting ; reproduced from [8] © 2011 IEEE.

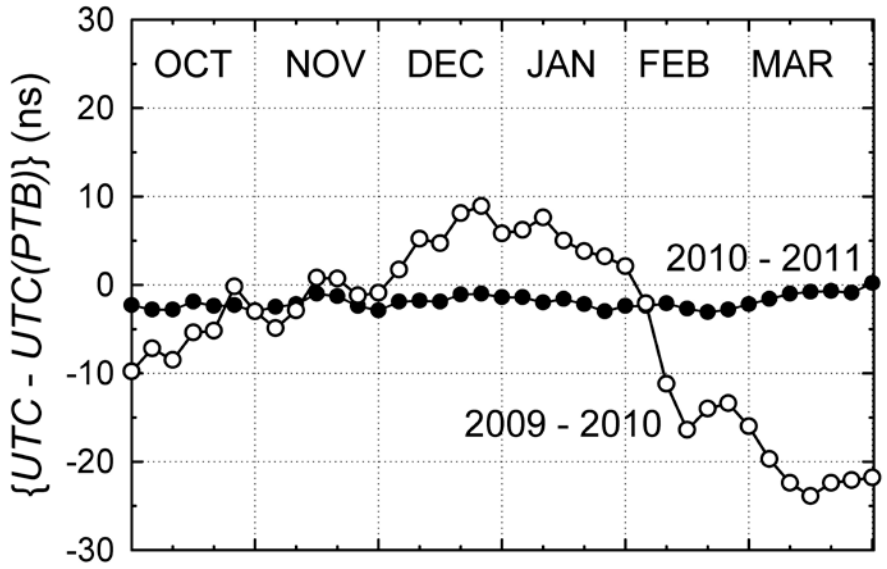

Figure 6. Six months time scale comparison UTC-UTC(PTB) in 2009 - 2010 and 2010 – 2011, respectively; reproduced from [8] © 2011 IEEE.

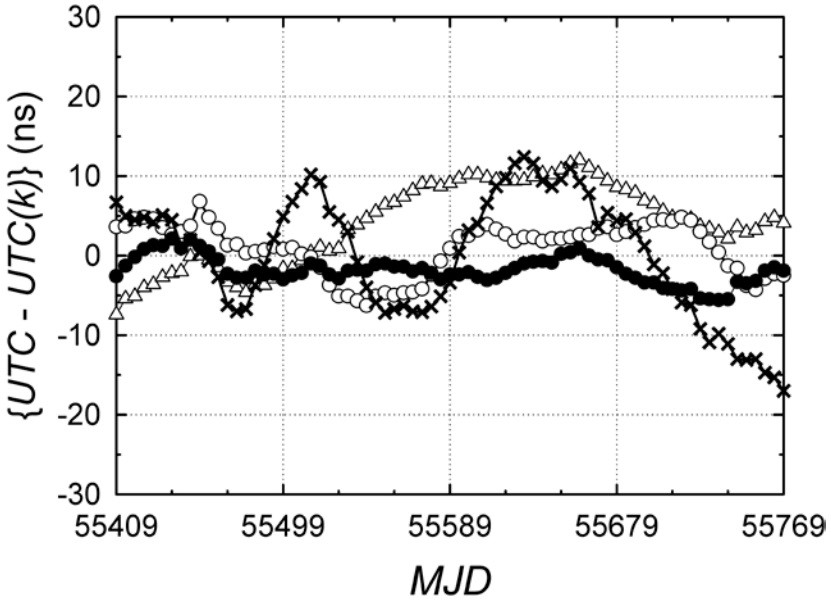

Figure 7. Time scale comparison UTC-UTC(k) during one year, including July 2011; k = NIST (triangles), k = USNO (open circles), k = SU (crosses), k = PTB (full circles).

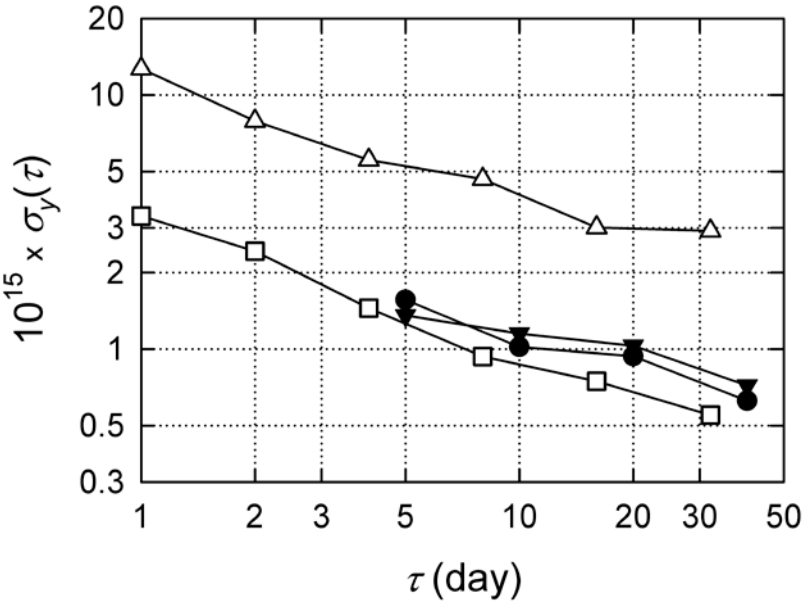

Figure 8. Relative frequency instability $\sigma_y(\tau)$ calculated from the time scale differences UTC(PTB)-UTC(NIST), based on daily averaged TWSTFT measurements: MJD 55043-55343, CS2-based (open triangles), and MJD 55447-55747, maser and fountain based (open squares); UTC-UTC(PTB) (full circles) and UTC-UTC(NIST) (full triangles) during MJD 55409 - 55769.

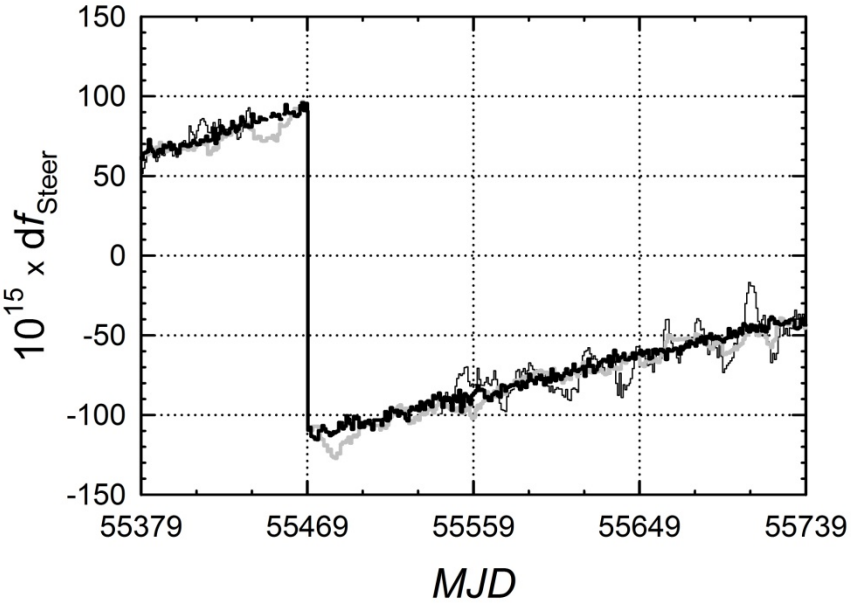

Figure 9. Three optional values of δf_{Steer} calculated during one year including June 2011; Option 1 (bold black line), Option 2 (grey line), Option 3 (thin black line), based on CS2 with a gap in the data because of the interruption of its operation in autumn 2010.

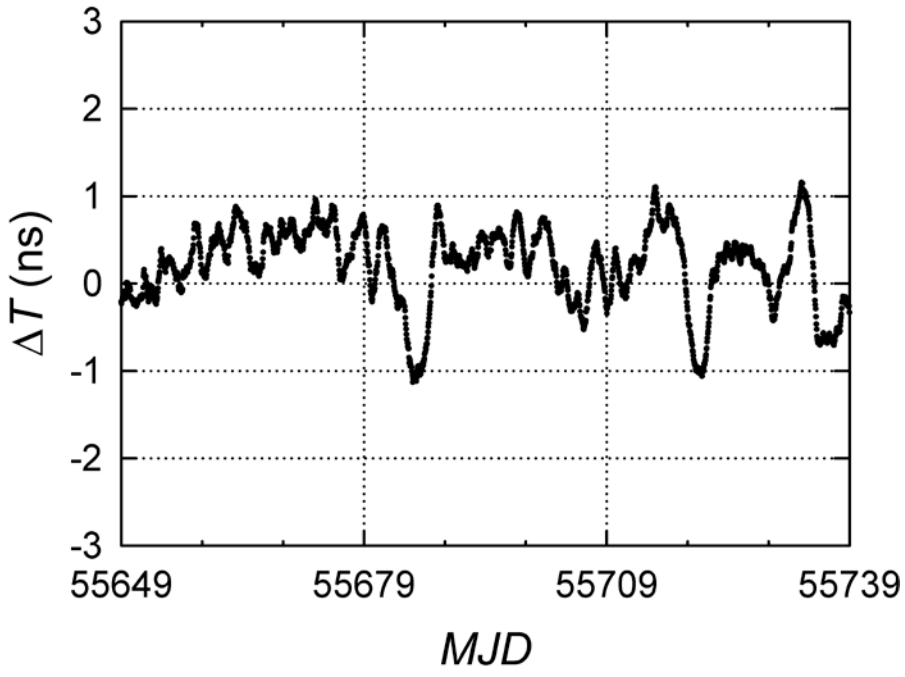

Figure 10. ΔT: = {*UTH(PTB) –UTC(PTB)*} during three months including June 2011.

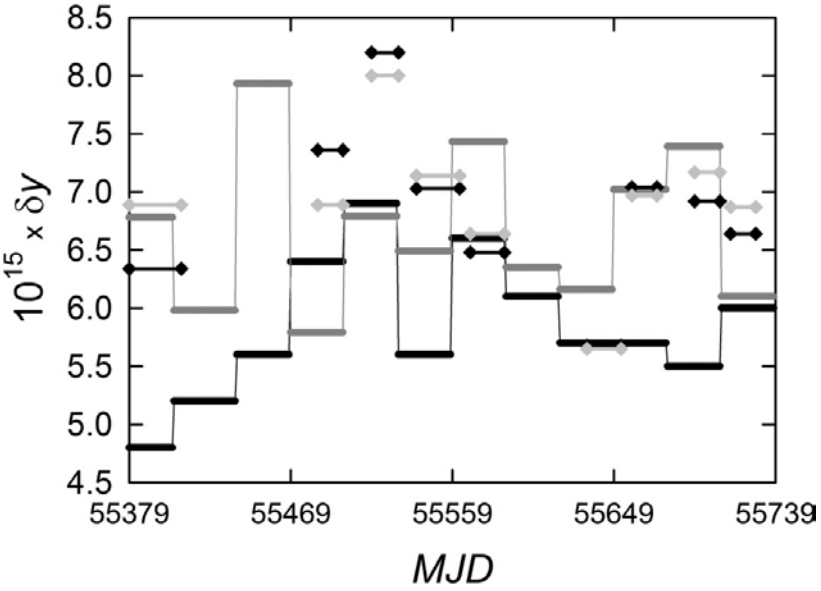

Figure 11. Four options to estimate the relation between CSF1 and the rate of TAI: Monthly reported value *d* from Circular T, Section 4, which was actually used as δf_{Rate} (connected black bars), reported values *d*(CSF1) for periods when CSF1 is used to measure the TAI scale unit (isolated black bars), d_1(CSF1) as described in the text (connected grey bars), d_2(CSF1) as explained in the text (isolated dark grey bars).

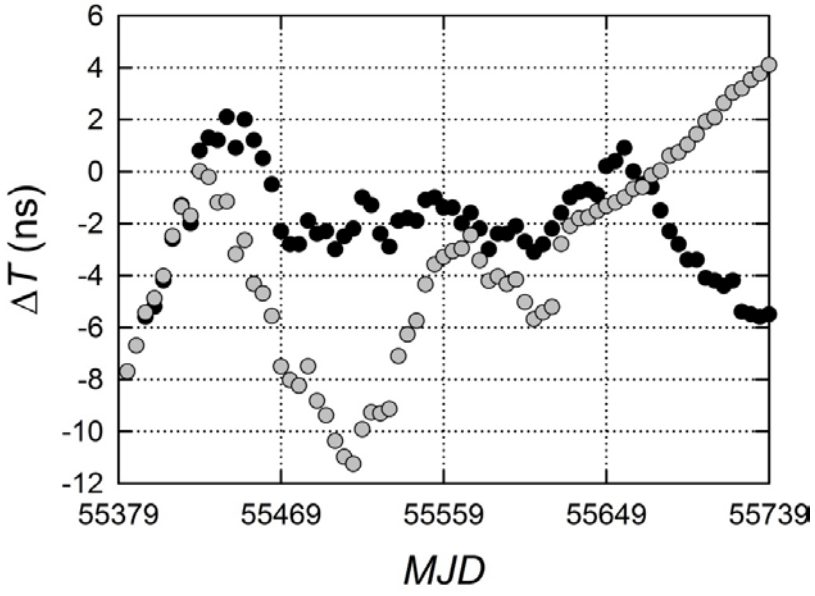

Figure 12. Deviation of UTC(PTB) from UTC: as actually reported in Circular T (black), fictively calculated (grey) as described in the text, based on the monthly values d_1(CSF1) (grey in Figure 11).

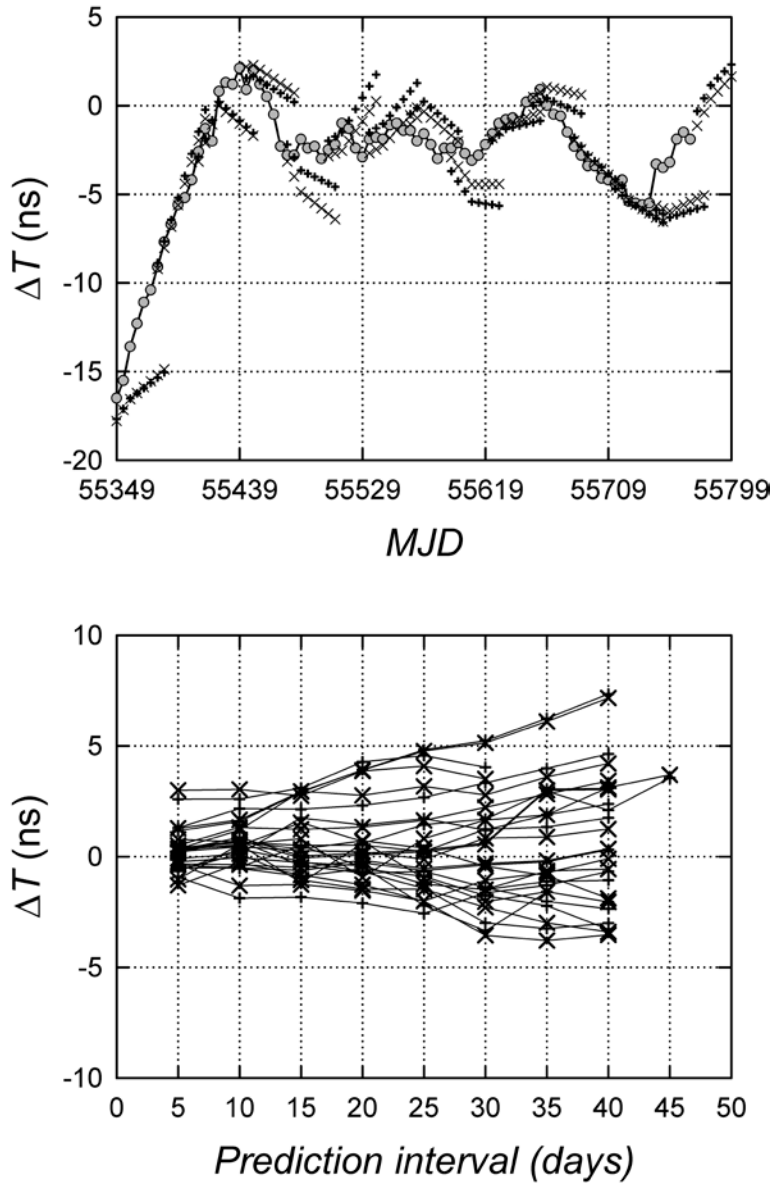

Figure 13. Prediction of UTC-UTC(PTB) during 15 months including August 2011 using two methods of transferring information from one month to the other: LF (symbol +) and LPR (symbol ×), see text for explanations; real data together with predictions (upper), differences between prediction and data available one month later (lower, only up to July 2011). Since Circular T is published usually after the 10th of a calendar month, the prediction over 5 and 10 days is mostly irrelevant and shown only for completeness.